Global warming shifts Pacific tropical cyclone location

Tim Li,[1] MinHo Kwon,[1,3] Ming Zhao,[3] Jong-Seong Kug,[2] Jing-Jia Luo,[4] and Weidong Yu[5]

Received 23 August 2010; accepted 21 September 2010; published 3 November 2010.

[1] A global high-resolution (~40 km) atmospheric general circulation model (ECHAM5 T319) is used to investigate the change of tropical cyclone frequency in the North Pacific under global warming. A time slice method is used in which sea surface temperature fields derived from a lower-resolution coupled model run under the 20C3M (in which historical greenhouse gases in 20th century were prescribed as a radiative forcing) and A1B (in which carbon dioxide concentration was increased 1% each year from 2000 to 2070 and then was kept constant) scenarios are specified as the lower boundary conditions to simulate the current and the future warming climate, respectively. A significant shift is found in the location of tropical cyclones from the western to central Pacific. The shift to more tropical cyclones in the central and less in the western Pacific is not attributable to a change in atmospheric static stability, but to a change in the variance of tropical synoptic-scale perturbations associated with a change in the background vertical wind shear and boundary layer divergence. **Citation:** Li, T., M. Kwon, M. Zhao, J.-S. Kug, J.-J. Luo, and W. Yu (2010), Global warming shifts Pacific tropical cyclone location, *Geophys. Res. Lett.*, *37*, L21804, doi:10.1029/2010GL045124.

1. Introduction

[2] Tropical cyclones (TC) are among the most devastating weather phenomena that can affect human life and economy. How global warming will affect TC activity is a hotly debated topic [*Webster et al.*, 2005; *Emanuel*, 2005; *Landsea et al.*, 2006]. It has been long recognized that TC genesis depends on sea surface temperature (SST) because a higher SST provides TCs with high ocean thermal energy. In addition to SST, TC genesis also depends on other dynamic and thermodynamic conditions such as atmospheric static stability, humidity, perturbation strength, and vertical wind shear [*Gray*, 1979; *Wu and Lau*, 1992; *Emanuel and Nolan*, 2004]. Particularly in the western North Pacific, atmospheric circulation patterns rather than local SST play an important role in interannual and interdecadal timescales [*Chan*, 2000; *Matsuura et al.*, 2003; *Ho et al.*, 2004] and future projection [*Yokoi and Takayabu*, 2009].

[3] TCs originate from tropical disturbances. Statistically, only a small percentage of the tropical disturbances eventually develop into TCs. With the increase of the global SST and surface moisture, it is anticipated that more TCs would develop. However, many climate models simulate a global decreasing trend of TC frequency [*Sugi et al.*, 2002; *McDonald et al.*, 2005; *Hasegawa and Emori*, 2005; *Yoshimura et al.*, 2006; *Oouchi et al.*, 2006; *Bengtsson et al.*, 2007]. One explanation of the decrease of TC frequency is attributed to an increase of atmospheric static stability. This is because the global warming leads to a larger increase of air temperature in the upper troposphere than in the lower troposphere; as a result, the atmosphere becomes more stable, which suppresses the TC frequency [*Sugi et al.*, 2002; *Bengtsson et al.*, 2007]. If this is true and it dominates the regional change of TC frequency, then one would expect the decrease of TC frequency throughout all ocean basins. However, as shown by this study, there are opposite trends of TC frequency between the western and central Pacific.

[4] A concept of a relative SST warming was introduced recently to explain the change of basin-wide TC frequency under global warming [e.g., *Swanson*, 2008; *Vecchi et al.*, 2008; *Knutson et al.*, 2008; *Zhao et al.*, 2009, 2010]. In particular, *Zhao et al.* [2009] found that both the present-day inter-annual variability of Atlantic hurricane frequency and the inter-model spread in their simulated frequency response of hurricanes to 21st century global warming projections (based on the IPCC AR4 models) can be well explained by a relative SST index defined as the SST difference between the Atlantic Main Development Region and the global tropical mean. While this result suggests that the large-scale dynamic and thermodynamic conditions that are relevant to TC genesis are closely tied to spatial distributions of SST in the Atlantic and eastern Pacific [*Zhao et al.*, 2010], such a simple relative SST index fails in explaining the change in the western Pacific. It is worth mentioning that the relative SST concept implies the importance of changes in atmospheric circulation in response to the change of SST distribution in affecting future TC frequency.

[5] This study investigates the cause of shift of TC genesis locations in the Pacific in a warmer climate based on a high-resolution atmospheric general circulation model (AGCM). In the following, we first introduce the model and numerical experiments, and then we discuss the model results, with a focus on the shift of TC location and associated characteristics of mean state changes. Finally, we summarize the main finding of this study.

2. Methodology and Model Description

[6] AGCM used in this study is ECHAM5 [*Roeckner et al.*, 2003] at a horizontal resolution of T319 (about 40-km grid). This high-resolution global model is run at Japan's Earth

[1]International Pacific Research Center, University of Hawaii at Manoa, Honolulu, Hawaii, USA.
[2]Korea Ocean Research and Development Institute, Ansan, South Korea.
[3]GFDL, NOAA, Princeton, New Jersey, USA.
[4]Research Institute for Climate Change, JAMSTEC, Yokohama, Japan.
[5]First Institute of Oceanography, State Oceanic Administration, China.

0094-8276/10/2010GL045124

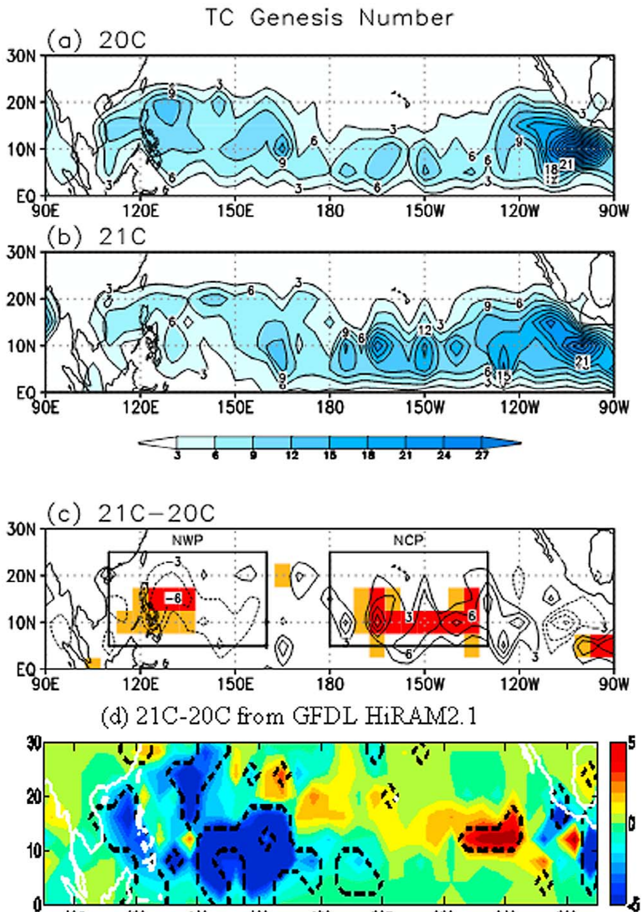

Figure 1. TC genesis number at each 2.5° × 2.5° box for a 20-year period derived from T319 ECHAM5 for (a) 20C, (b) 21C, and (c) difference between Figures 1b and 1a (21C-20C). In Figure 1c red (orange) shaded areas indicate 95% (90%) confidence level. (d) Same as Figure 1c except from the GFDL HiRAM2.1 model with an ensemble SST pattern averaged from 18 IPCC-AR4 models (dashed line denotes the 95% confidence level).

Simulator. SST, the lower boundary condition of the model, is derived from a lower-resolution (T63) coupled version of the model (ECHAM5/MPI-OM) [*Jungclaus et al.*, 2006], which participated in the fourth assessment report of intergovernmental panel for climate change (IPCC-AR4). Two different climate change scenarios (20C3M and A1B) were applied. In 20C3M scenario, increasing historical greenhouse gases in 20th century were prescribed as a radiative forcing. In A1B scenario, carbon dioxide concentration was increased at a rate 1% per year till it reached 720 ppm and was then kept constant. A 'time-slice' method [*Bengtsson et al.*, 1996] was applied, in which the high-resolution AGCM is forced by SST during two 20-year periods (1980–1999 and 2080–2099). The two periods are hereafter referred to as 20C and 21C, respectively.

[7] Following *Thorncroft and Hodges* [2001], TCs in the model are determined based on the following three criteria: 1) 850-hPa vorticity is greater than 1.75×10^{-5} s^{-1}, 2) warm core strength (represented by the difference between 850 and 250 hPa vorticity) exceeds 0.8×10^{-5} s^{-1}, and 3) duration time exceeds 2 days. The selection of the parameter values is based on the least square fitting of the observed TC number in northern hemisphere in 20C.

3. Results

[8] Figure 1 shows the geographical distribution of TC genesis locations in the Pacific in the 20C and 21C simulations. In 20C, TCs form primarily over the western and eastern Pacific, similar to the distribution of the observed genesis locations [*Gray*, 1979]. In 21C, however, more TCs shift their genesis locations to the Central Pacific. As seen from the difference map (Figure 1c), there are two notable TC decrease and increase regions over the Pacific. One is over the North western Pacific (NWP) and the other the North central Pacific (NCP). The numbers of TCs in 21C decreases by 31% over NWP but increases by 65% over NCP. Thus the high-resolution AGCM simulations illustrate two opposite TC trends in NWP and NCP.

[9] To demonstrate that the result above is not a specific feature of the ECHAM5 model and its projected SST warming pattern, we also examined the simulation results from the GFDL global 50-km resolution AGCM (HiRAM2.1, for detailed model description and its realistic simulation of the annual, inter-annual and decadal variations of TC activity, readers are referred to *Zhao et al.* [2009]) with an ensemble SST warming pattern from 18 IPCC AR4 models [*Zhao et al.*, 2009]. The two models have different treatments in various physical parameterization schemes. For example, in convective heating parameterization ECHAM5 uses a mass flux scheme while HiRAM2.1 uses a modified *Bretherton et al.* [2004] scheme. Figure 1d shows the difference in TC genesis number between 21C and 20C from the GFDL model. An opposite TC trend can also be seen between NWP and NCP, supporting the ECHAM5 result.

[10] To understand the cause of this distinctive shift in TC location with global warming, we diagnose the dynamic and thermodynamic conditions in northern summer (July–October, when a majority of TCs occur) over the NWP (5–25°N, 110°E-160°E) and NCP (5–25°N, 180–130°W) regions. First we examine the change of atmospheric stability. Figures 2a and 2b show the vertical profiles of the atmospheric potential and equivalent potential temperatures averaged over NWP and NCP. The upper-level air temperature increases at a greater rate than that at lower levels in both the regions. As the static stability is measured by the vertical gradient of the potential temperature, the result implies that the atmosphere becomes more stable under the global warming in both the regions. Due to the effect of atmospheric humidity (which increases more in the lower troposphere), the vertical gradient of equivalent potential temperature approximately remains same from 20C to 21C. This implies that the atmospheric convective instability remains unchanged in both the regions. Thus, both the static stability and the convective instability changes cannot explain the opposite trends of TC frequency between NWP and NCP.

[11] A further analysis reveals that the fundamental cause of the opposite TC trends lies in the change of dynamic conditions. As we know, TCs originate from the tropical disturbances such as synoptic wave trains and easterly waves [e.g., *Lau and Lau*, 1990; *Li et al.*, 2003; *Tam and Li*, 2006; *Fu et al.*, 2007]. The 21C simulation shows an increased

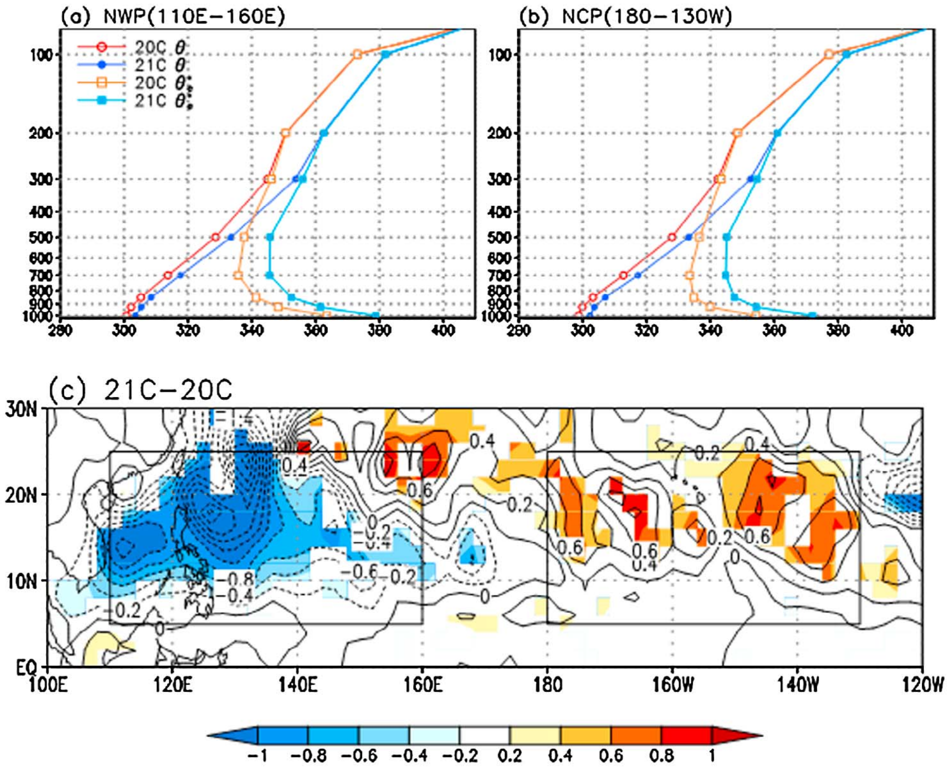

Figure 2. Vertical profiles of potential and equivalent potential temperatures (unit: K) at 20C and 21C averaged over (a) NWP and (b) NCP and the variance difference (c) of synoptic-scale (2-8-day) vorticity at 850 hPa (unit: 10^{-10} s^{-2}) in northern summer (July–October) between 21C and 20C, with shaded areas indicating a 95% confidence level or above (with an F test).

variability of synoptic-scale disturbances over the NCP region but a decreased synoptic activity over the NWP region. Here the strength of the synoptic-scale disturbances is represented by the variance of the 850-hPa vorticity field that is filtered at a 2-8 day band using Lanzcos digital filter [*Duchon*, 1979]. The difference map (Figure 2c) shows a remarkable decrease of the synoptic-scale variance over (10–20N, 110–140E) but an increase of the variance in (10–20N, 180–130W). The importance of synoptic activity on future projection of TC genesis frequency was also pointed out by *Yokoi and Takayabu* [2009]. Thus, the decreasing trend in NWP is caused by the reduced synoptic-scale activity whereas the increasing trend in NCP is caused by the strengthening of synoptic disturbances.

[12] We argue here that the contrast of the synoptic-scale activity between NWP and NCP results from the change of the background vertical wind shear (Figure 3a) and low-level divergence (Figure 3c). It has been pointed out that the easterly shear and low-level convergence of the background mean flow favor the development of tropical disturbances [*Wang and Xie*, 1996; *Li*, 2006; *Sooraj et al.*, 2008]. In the 20C simulation, the western Pacific and Indian monsoon regions have a prevailing easterly wind shear in association with large-scale convective heating. This easterly wind shear becomes weaker in the warming climate (Figure 3a). The weakening of the easterly wind shear corresponds to a weakened western Pacific monsoon, as seen from Figure 3b. The weakening of the easterly shear, along with low-level divergence to its east (Figure 3c), further suppresses the development of tropical disturbances in NWP. In contrast, the easterly shear and low-level convergence in NCP are strengthened, and so is the precipitation (Figure 3). They favor the development of tropical disturbances in NCP.

[13] What causes the change of the vertical shear and the low-level divergence? We argue that the change of the background vertical shear and the low-level divergence is closely related to changes of the trade wind in the tropics (Figure 3c). Many IPCC-AR4 models predict an El Nino-like warming pattern in the Pacific under the global warming climate state [*Intergovernmental Panel on Climate Change*, 2007], that is, a greater SST warming occurs in the tropical eastern and central Pacific compared to that in the tropical western Pacific. As a result, the zonal SST gradient is reduced across the tropical Pacific. The reduced zonal SST gradient decreases the trade wind [*Lindzen and Nigam*, 1987] and weakens the Walker circulation. Furthermore, GCM simulations with a uniform SST warming also produce a weakening of the Walker circulation, which can be understood in terms of the energy and mass balance of the ascending branch of the circulation [*Held and Soden*, 2006; *Vecchi et al.*, 2006]. Therefore, both the reduced zonal SST gradient and the global mean SST warming decrease the trade wind.

[14] The weakening of the trades leads to, on the one hand, the decrease of the boundary-layer convergence in the western Pacific monsoon region and, on the other hand, the increase of the boundary layer convergence in NCP (Figure 3c). The former suppresses the monsoon convective heating and decreases the easterly shear in NWP, whereas the latter

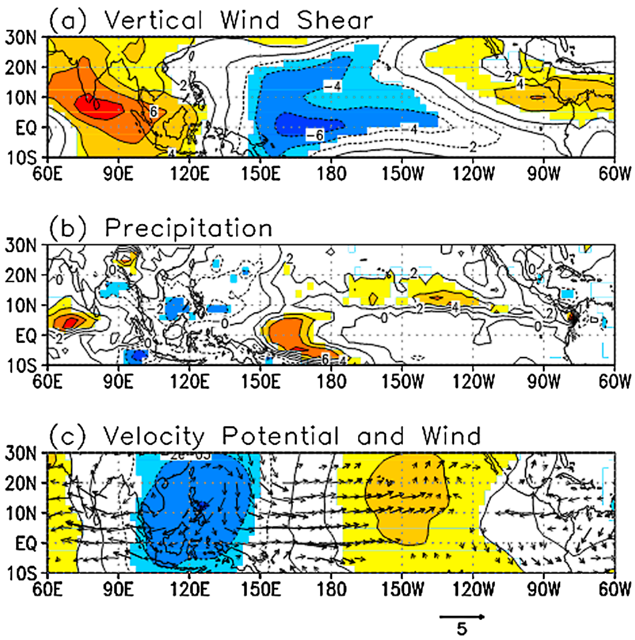

Figure 3. Difference (21C–20C) fields of (a) the vertical shear of zonal wind (200 hPa minus 850 hPa, unit: m s^{-1}), (b) precipitation (unit: mm day^{-1}), and (c) velocity potential (unit: s^{-1}) and wind (unit: m s^{-1}) at 850 hPa during northern summer (July–October). Areas that exceed the 95% confidence level (Student's *t* test) are shaded (for contour) and plotted (for vector).

strengthens the local boundary layer moisture convergence and convective heating and thus increases the easterly wind shear in NCP.

4. Summary and Discussion

[15] The shift of TC location in the Pacific due to the global warming is investigated using a high-resolution (~40 km) global AGCM (ECHAM5). It is noted that TC genesis number decreases significantly in the western Pacific but increases remarkably in the central tropical Pacific. Such a feature is also seen in the GFDL HiRAM2.1 forced with an IPCC-AR4 ensemble SST warming pattern.

[16] The cause of the two opposite TC trends is investigated. As the atmospheric static stability increases in both the regions under global warming, this stability control mechanism cannot explain the increasing trend over the central Pacific. The major factor that accounts for the distinctive opposite TC trends lies in the dynamic condition in the atmosphere. It is the change of strength of synoptic disturbances that is primarily responsible for the distinctive changes in the TC frequency between the western and central Pacific.

[17] Physical processes responsible for the distinctive TC frequency changes in the warming climate are discussed below. The global warming weakens the trade winds in the Pacific through both the effect of the uniform warming and the decrease of zonal SST gradients across the tropical Pacific. In the western Pacific, the weakened Walker circulation causes the anomalous boundary layer divergence that leads to a weakening of the western North Pacific monsoon rainfall. The weakening of the monsoon heating further causes a decrease in the background easterly shear. The decreased easterly shear and associated weakening of the low-level convergence to its east reduce the synoptic activity and thus decrease the TC genesis frequency. In contrast, in the central Pacific, an anomalous boundary layer convergence is induced due to the reduced SST gradient and higher local SST. This enhances the atmospheric convection and induces the easterly shear in situ. The easterly shear and the low-level convergence favor the growth of the synoptic disturbances, resulting in a TC frequency increase in the future warming climate.

[18] Projection on future cyclogenesis frequency is subject to a wide range of uncertainties including uncertainties in model physics and SST warming patterns [*Knutson et al.*, 2010]. Because ECHAM5 tends to overestimate TC genesis frequency in the central Pacific in 20C, a caution is needed to interpret the model results. The shift of projected TC activity in the Pacific may pose a great threat to millions' people living in Hawaii and central Pacific islands.

[19] **Acknowledgments.** This work was supported by ONR grants N000140810256 and N000141010774 and NRL grant N00173-09-1-G008 and by the International Pacific Research Center that is sponsored by the Japan Agency for Marine-Earth Science and Technology (JAMSTEC), NASA (NNX07AG53G) and NOAA (NA17RJ1230). MK was supported by KORDI grant PE98537. This is SOEST contribution 8016 and IPRC contribution 720.

References

Bengtsson, L., M. Botzet, and M. Esch (1996), Will greenhouse gas-induced warming over the next 50 years lead to higher frequency and greater intensity of hurricanes?, *Tellus, Ser. A*, *48*, 57–73, doi:10.1034/j.1600-0870.1996.00004.x.

Bengtsson, L., K. I. Hodges, M. Esch, N. Keenlyside, L. Komblush, J. J. Luo, and T. Yamagata (2007), How many tropical cyclones change in a warmer climate, *Tellus, Ser. A*, *59*, 539–561, doi:10.1111/j.1600-0870.2007.00251.x.

Bretherton, C. S., J. R. McCaa, and H. Grenier (2004), A new parameterization for shallow cumulus convection and its application to marine subtropic cloud-topped boundary layers. Part I: Description and 1D results, *Mon. Weather Rev.*, *132*, 864–882, doi:10.1175/1520-0493(2004)132<0864:ANPFSC>2.0.CO;2.

Chan, J. C. L. (2000), Tropical cyclone activity over the western North Pacific associated with El Niño and La Niña events, *J. Clim.*, *13*, 2960–2972, doi:10.1175/1520-0442(2000)013<2960:TCAOTW>2.0.CO;2.

Duchon, C. E. (1979), Lanczos filtering in one and two dimensions, *J. Appl. Meteorol.*, *18*, 1016–1022, doi:10.1175/1520-0450(1979)018<1016:LFIOAT>2.0.CO;2.

Emanuel, K. A. (2005), Increasing destructiveness of tropical cyclones over the past 30 years, *Nature*, *436*, 686–688, doi:10.1038/nature03906.

Emanuel, K. A., and D. S. Nolan (2004), Tropical cyclone activity and global climate, in *Proceedings of the 26th Conference on Hurricanes and Tropical Meteorology*, pp. 240–241., Am. Meteorol. Soc., Miami, Fla.

Fu, B., T. Li, M. Peng, and F. Weng (2007), Analysis of tropical cyclone genesis in the western North Pacific for 2000 and 2001, *Weather Forecasting*, *22*, 763–780.

Gray, W. M. (1979), Hurricanes: Their formation, structure and likely role in the tropical circulation, in *Meteorology over the Tropical Oceans*, edited by D. B. Shaw, pp. 155–218, R. Meteorol. Soc., Bracknell, U. K.

Hasegawa, A., and S. Emori (2005), Tropical cyclones and associated precipitation over the western North Pacific: T106 atmospheric GCM simulation for present-day and doubled CO_2 climates, *SOLA*, *1*, 145–148, doi:10.2151/sola.2005-038.

Held, I. M., and B. J. Soden (2006), Robust responses of the hydrological cycle to global warming, *J. Clim.*, *19*, 5686–5699, doi:10.1175/JCLI3990.1.

Ho, C.-H., J.-J. Baik, J.-H. Kim, D.-Y. Gong, and C.-H. Sui (2004), Interdecadal changes in summertime typhoon tracks, *J. Clim.*, *17*, 1767–1776, doi:10.1175/1520-0442(2004)017<1767:ICISTT>2.0.CO;2.

Intergovernmental Panel on Climate Change (2007), *Climate Change 2007: The Physical Science Basis. Contribution of Working Group I to the Fourth Assessment Report of the Intergovernemental Panel on Climate Change*, edited by S. Solomon et al., Cambridge Univ. Press, Cambridge, U. K.

Jungclaus, H., et al. (2006), Ocean circulation and tropical variability in the coupled model ECHAM5/MPO-OM, *J. Clim.*, *19*, 3952–3972, doi:10.1175/JCLI3827.1.

Knutson, T., J. Sirutis, S. Garner, G. A. Vecchi, and I. M. Held (2008), Simulated reduction in Atlantic hurricane frequency under twenty-first-century warming condition, *Nat. Geosci.*, *1*, 359–364, doi:10.1038/ngeo202.

Landsea, C. W., B. A. Harper, K. Hoarau, and J. A. Knaff (2006), Can we detect trends in extreme tropical cyclones?, *Science*, *313*, 452–454, doi:10.1126/science.1128448.

Lau, K.-H., and N.-C. Lau (1990), Observed structure and propagation characteristics of tropical summertime synoptic-scale disturbances, *Mon. Weather Rev.*, *118*, 1888–1913, doi:10.1175/1520-0493(1990)118<1888:OSAPCO>2.0.CO;2.

Li, T. (2006), Origin of the summertime synoptic-scale wave train in the western North Pacific, *J. Atmos. Sci.*, *63*, 1093–1102, doi:10.1175/JAS3676.1.

Li, T., B. Fu, X. Ge, B. Wang, and M. Peng (2003), Satellite data analysis and numerical simulation of tropical cyclone formation, *Geophy. Res. Lett.*, 2122–2126.

Lindzen, R. S., and S. Nigam (1987), On the role of sea surface temperature gradients in forcing low level winds and convergence in the tropics, *J. Atmos. Sci.*, *44*, 2418–2436, doi:10.1175/1520-0469(1987)044<2418:OTROSS>2.0.CO;2.

Matsuura, T., M. Yumoto, and S. Iizuka (2003), A mechanism of interdecadal variability of tropical cyclone activity over the western North Pacific, *Clim. Dyn.*, *21*, 105–117, doi:10.1007/s00382-003-0327-3.

McDonald, R. E., et al. (2005), Tropical storms: Representation and diagnosis in climate models and the impacts of climate change, *Clim. Dyn.*, *25*, 19–36, doi:10.1007/s00382-004-0491-0.

Oouchi, K., et al. (2006), Tropical cyclone climatology in a global-warming climate as simulated in a 20km-mesh global atmospheric model: Frequency and wind intensity analyses, *J. Meteorol. Soc. Jpn.*, *84*, 259–276, doi:10.2151/jmsj.84.259.

Roeckner, E., et al. (2003), The atmospheric general circulation model ECHAM5. Part I: Model description, *Rep. 349*, 127 pp., Max Planck Inst. for Meteorol, Hamburg, Germany.

Sooraj, K. P., D. Kim, J.-S. Kug, S.-W. Yeh, F.-F. Jin, and I.-S. Kang (2008), Effects of the low frequency zonal wind variation on the high-frequency atmospheric variability over the tropics, *Clim. Dyn.*, *33*, 496–507, doi:10.1007/s00382-008-0483-6.

Sugi, M., A. Noda, and N. Sato (2002), Influence of the global warming on tropical cyclone climatology: An experiment with the JMA global model, *J. Meteorol. Soc. Jpn.*, *80*, 249–272, doi:10.2151/jmsj.80.249.

Swanson, K. L. (2008), Nonlocality of Atlantic tropical cyclone intensities, *Geochem. Geophys. Geosyst.*, *9*, Q04V01, doi:10.1029/2007GC001844.

Tam, C.-Y., and T. Li (2006), The origin and dispersion characteristics of the observed summertime synoptic-scale waves over the western Pacific, *Mon. Wea. Rev.*, *134*, 1630–1646.

Thorncroft, C., and K. Hodges (2001), African easterly wave variability and its relationship to Atlantic tropical cyclone activity, *J. Clim.*, *14*, 1166–1179, doi:10.1175/1520-0442(2001)014<1166:AEWVAI>2.0.CO;2.

Vecchi, G. A., B. J. Soden, A. T. Wittenberg, I. M. Held, A. Leetmaa, and M. J. Harrison (2006), Weakening of tropical Pacific atmospheric circulation due to anthropogenic forcing, *Nature*, *441*, 73–76, doi:10.1038/nature04744.

Vecchi, G. A., K. Swanson, and B. Soden (2008), Whither hurricane activity, *Science*, *322*, 687–689, doi:10.1126/science.1164396.

Wang, B., and X. Xie (1996), Low-frequency equatorial waves in sheared zonal flow. Part I: Stable waves, *J. Atmos. Sci.*, *53*, 449–467, doi:10.1175/1520-0469(1996)053<0449:LFEWIV>2.0.CO;2.

Webster, P. J., G. J. Holland, J. A. Curry, and H.-R. Chang (2005), Changes in tropical cyclone number, duration, and intensity in a warming environment, *Science*, *309*, 1844–1846, doi:10.1126/science.1116448.

Wu, G., and N.-C. Lau (1992), A GCM simulation of the relationship between tropical-storm formation and ENSO, *Mon. Weather Rev.*, *120*, 958–977, doi:10.1175/1520-0493(1992)120<0958:AGSOTR>2.0.CO;2.

Yokoi, S., and Y. N. Takayabu (2009), Multi-model projection of global warming impact on tropical cyclone genesis frequency over the western North Pacific, *J. Meteorol. Soc. Jpn.*, *87*, 525–538, doi:10.2151/jmsj.87.525.

Yoshimura, J., M. Sugi, and A. Noda (2006), Influence of greenhouse warming on tropical cyclone frequency, *J. Meteorol. Soc. Jpn.*, *84*, 405–428, doi:10.2151/jmsj.84.405.

Zhao, M., I. M. Held, S.-J. Lin, and G. A. Vecchi (2009), Simulations of global hurricane climatology, interannual variability, and response to global warming using a 50 km resolution GCM, *J. Clim.*, *22*, 6653–6678, doi:10.1175/2009JCLI3049.1.

Zhao, M., I. M. Held, and G. A. Vecchi (2010), Retrospective forecasts of the hurricane season using a global atmospheric model assuming persistence of SST anomalies, *Mon. Weather Rev.*, doi:10.1175/2010MWR3366.1, in press.

J.-S. Kug, Korea Ocean Research and Development Institute, 1270 Sa-dong Sangnok-gu, Ansan, Gyeonggi 426-744, South Korea.

M. Kwon and T. Li, International Pacific Research Center, University of Hawaii at Manoa, 1680 East-West Rd., Honolulu, HI 96822, USA. (timli@hawaii.edu)

J.-J. Luo, Research Institute for Climate Change, JAMSTEC, 3173-25 Showa-machi, Kanazawa-ku, Yokohama, Kanagawa 236-0001, Japan.

W. Yu, First Institute of Oceanography, State Oceanic Administration, 6, Road Xian-Xia-Ling, Qingdao, Shandong 266061, China.

M. Zhao, GFDL, NOAA, PO Box 308, Princeton, NJ 08542, USA.